Compact Liquid Crystal Waveguide Based Fourier Transform Spectrometer for In-Situ and Remote Gas and Chemical Sensing

Tien-Hsin Chao, Thomas T. Lu,
Jet Propulsion Laboratory
4800 Oak Grove Drive, Pasadena CA, 91109

Scott R. Davis, Scott D. Rommel, George Farca, Ben Luey, Alan Martin, Michael H. Anderson
Vescent Photonics Inc.
4865 E. 41st Ave, Denver CO, 80216

Key Words: Solid-state Fourier transform spectrometer, liquid crystal waveguide, miniature spectrometer, near-IR spectrometer, liquid crystal clad waveguide, electro-optic FTIR

ABSTRACT

Vescent Photonics Inc. and Jet Propulsion Lab are jointly developing an innovative ultra-compact (volume < 10 cm^3), ultra-low power (<10^{-3} Watt-hours per measurement and zero power consumption when not measuring), **completely non-mechanical** electro-optic Fourier transform spectrometers (EO-FTS) that will be suitable for a variety of remote-platform, in-situ measurements. These devices are made possible by a novel electro-evanescent waveguide architecture, enabling "chip-scale" EO-FTS sensors. The potential performance of these EO-FTS sensors include: i) a spectral range throughout 0.4-5 μm (25000 – 2000 cm^{-1}), ii) high-resolution ($\Delta\lambda \leq 0.1$ nm), iii) high-speed (< 1 ms) measurements, and iv) rugged integrated optical construction. This performance potential enables the detection and quantification of a large number of different atmospheric gases simultaneously in the same air mass and the rugged construction will enable deployment on previously inaccessible platforms. The sensor construction is also amenable for analyzing aqueous samples on remote floating or submerged platforms. To date a proof-of-principle prototype EO-FTS sensor has been demonstrated in the near-IR (range of 1450-1700 nm) with a 5 nm resolution. This performance is in good agreement with theoretical models, which are being used to design and build the next generation of EO-FTS devices.

1. INTRODUCTION

The potency of Fourier transform spectroscopy (FTS) for chemical analysis is well established;{Davis, 2001 #11} it provides identification and quantification of multiple compounds (e.g., biogenically important CH_4, NH_4, NO_x, H_2O, and many more) with a high level of sensitivity (ppm for gas phase detection) and specificity (spectroscopic identification). Furthermore, FTS has proven advantages over other spectroscopic techniques (e.g. gratings, prisms, or variable filters) because of both the time-multiplexing effect (better S/N) and optical throughput (all of the photons are collected). As a testament to the utility of FTS the ATMOS instrument{ #407}, for example, measured over 30 different gases in the Earth's atmosphere plus over 20 isotopic variants. Furthermore, FTS provides the entire spectrum with each scan, and unlike grating based spectrometers the spectral resolution is not inversely related to the wavelength range. This "full-spectrum-at-once" attribute of FTS is especially suited for multicomponent analysis, where overlapping spectral features of numerous analytes can complicate concentration quantification. This can be especially advantageous when compared with limited wavelength range tunable laser approaches. Despite this utility, the use of FTS sensors on planetary rovers and other remote missions has been complicated by the opto-mechanical requirements for traditional scanning Michelson interferometers. Up till now, there has not been an electro-optic technology that provides sufficient control over optical phase. As will be shown, the EO-waveguide architecture presented here provides unprecedented voltage control over optical phase (> 1 mm demonstrated and up to 10 cm possible), orders of magnitude more than any other technology. This previously unrealizable level of control makes possible an entirely new type of FTS system.

Optical Pattern Recognition XIX, edited by David P. Casasent, Tien-Hsin Chao,
Proc. of SPIE Vol. 6977, 69770P, (2008) · 0277-786X/08/$18 · doi: 10.1117/12.785888

The essential elements of a traditional FTS absorbance sensor are shown in Figure 1. Very briefly, emission from a broadband light source, which is typically a heated element for the mid- to far-IR or a tungsten lamp in the near-IR, passes through the analyte and the interferometer (preferred order dependent upon application) prior to detection. FTS sensors may also work in solar occultation mode, wherein the sun provides a broadband light soure. The interferogram, i.e., intensity recorded by the detector as a function of the optical path difference (OPD) between the two arms of the interferometer, is digitized and Fourier transformed. This OPD is typically generated via a linear translation of a Michelson interferometer (see Fig. 1). This transform provides the full spectrum, which represents the broadband light source emission and detector sensitivity profiles modified with depleted regions arising from the analyte absorbance spectra. From analysis of this spectra constituent quantification is extracted. The extraordinary power of FTS arises from this ability to achieve detailed spectral information, over a broad region, from a single interferogram.

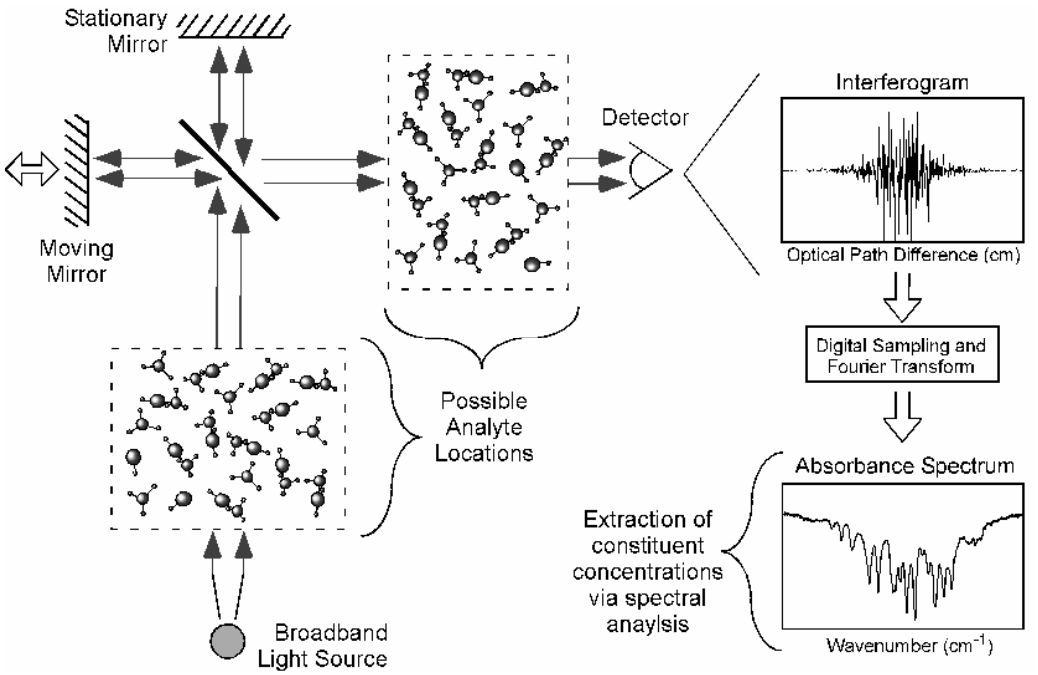

Figure 1: Schematic of the elements involved for constituent analysis via traditional FTS.

While the potency of FTS sensors is extremely well established with a long history of success, the moving mirror assembly provides size, weight, power and durability design challenges. This is especially true with the increased variety of future exploratory platforms including: flybys, orbiters, landers, airplanes or balloons in planetary atmospheres, Earth orbiting telescopes and sample return missions to various solar System bodies. Furthermore typical instruments have an onboard calibration laser to calibrate the linear motion, which further adds to the cost. An alternative technology free from this moving mirror assembly is therefore sought. Finally, for future NASA missions the moving mirror assembly provides specific challenges:

1) Over the course of a 5-year mission, tens of millions of strokes will be required, making wear or fatigue a serious risk

2) The moving optical element cannot be rigidly held, making it sensitive to vibration and requiring that it be "caged" during launch to prevent damage, adding risk (failure of the caging mechanism to reopen).

3) Accelerating and decelerating the optical elements can torque the spacecraft, making it difficult to maintain accurate pointing.

In principle electro-optics can be used to replace the moving mirror assembly.{Chao, 2005 #418} Figure 2 illustrates how the complicated opto-mechanical interferometer (left of Figure 2) may be replaced with a non-mechanical electro-optic medium. In typical electro-optic crystals, such at KTP or $LiNbO_3$, the birefringence of medium may be voltage tuned. If the input light is polarized at 45^o with respect to the crystal axis then the speed at which the two polarizations

propagate through the crystal may be voltage tuned. For a given length of crystal this translates into a voltage tunable optical path difference between the two polarizations. These two "arms" of the interferometer may then be recombined via another polarizer and a completely non-mechanical EO interferometer constructed. While this approach has long been known

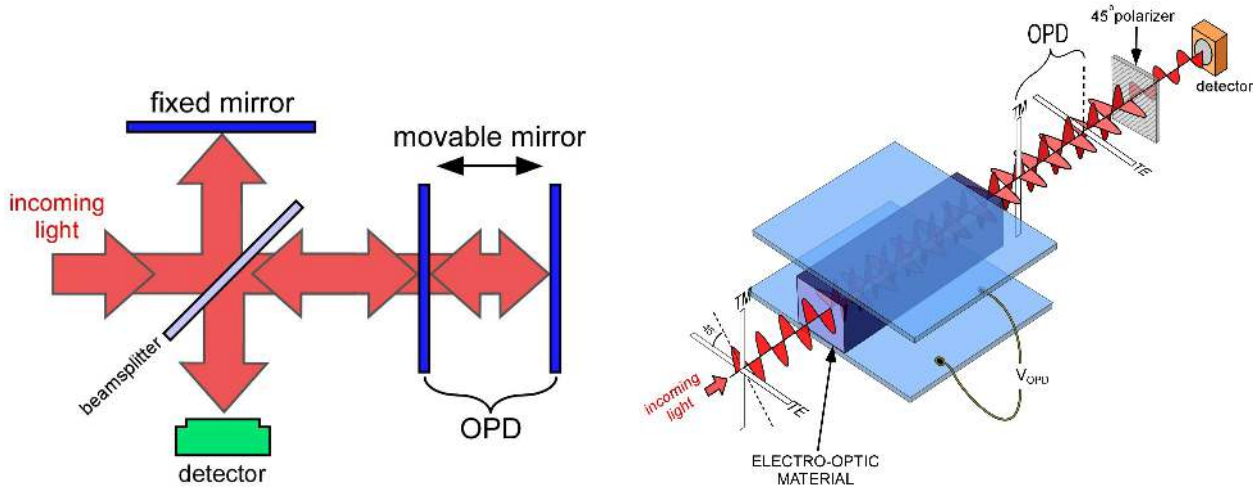

Figure 2. Optical path difference (OPD) techniques realized with a traditional Michelson interferometer (left); and a non-mechanical electro-optic approach (right).

the key challenge to replacing the opto-mechanics has been realizing an EO material that provides sufficient voltage tunability over OPD. Typical EO crystals realize only a few microns of tunability of OPD, which is suitable for intensity modulators but hardly provides a viable replacement for opto-mechanics. This is especially true for FTS applications, where the magnitude of OPD is inversely related to the spectral resolution. In the next section we will present our proprietary liquid crystal-waveguide architecture that provides unprecedented voltage tunability over OPD.

2. ELECTRO-OPTIC FOURIER TRANSFORM SPECTROMETER ON A CHIP

At Vescent Photonics we have invented and are developing a new electro-optic architecture that provides unprecedented voltage control over OPD (> 1 mm demonstrated and > 1 cm possible). This previously unrealizable level of control makes possible new devices with remarkable performance attributes. To date we have demonstrated: ultra-wide field of view (80^o) non-mechanical laser beamsteerers, chip-scale widely tunable lasers (nearly 40 nm tunability demonstrated), ultra-low power (< 5 μWatts) tunable micro-ring filters and Mach-Zehnder switches, and many more. All of these devices may be in small LCD-like packages that can ultimately be as low cost as a calculator display. In our work with JPL we have been using this architecture to build EO-FTS systems.

2.1. The Liquid Crystal Waveguide Architecture: Giant Voltage Control over OPD

Over the past several decades one of the most technically and commercially successful approaches for light control has been liquid-crystal (LC) optics. LCs have the world largest electro-optic response (Δn > 0.2 over 5 volts for a typical LC, which corresponds to 10^5-10^6 pm/V, i.e., several orders of magnitude larger than any other material), are environmentally stable, and inexpensive.{Khoo, 1993 #13} This has enabled the now > $50 billion a year display market. A typical "display-like" LC-optic is shown in Figure 3. The light traverses a thin (< 20 μm) LC layer that is sandwiched between glass sheets. Transparent electrodes are used to apply an electric field, which, in combination with polarizers, may be used to either block or transmit the light.

While undeniably potent for information displays, this traditional LC-optic has two significant limitations. First, the light must transmit through transparent electrodes, which in turn limits the total optical power that may be controlled. Second, and arguably more significant, the LC layer must be extremely thin. The LC- material is rendered a single-domain crystal via thin alignment layers. The LC-molecules that are adjacent these alignment layers are highly ordered, which means low scattering loss, and fast switching times. If one were to make the LC cell thicker, the bulk LC material would become prohibitively slow and opaque. Therefore, even though the LC material has a tremendous electro-optic effect, the necessarily short interaction length mitigates this effect. In order to circumvent these limitations we have invented and are developing the LC-clad waveguide architecture, as shown in Figure 4.{Anderson, 2005 #390; Anderson, 2006 #391; Anderson, 2006 #392}

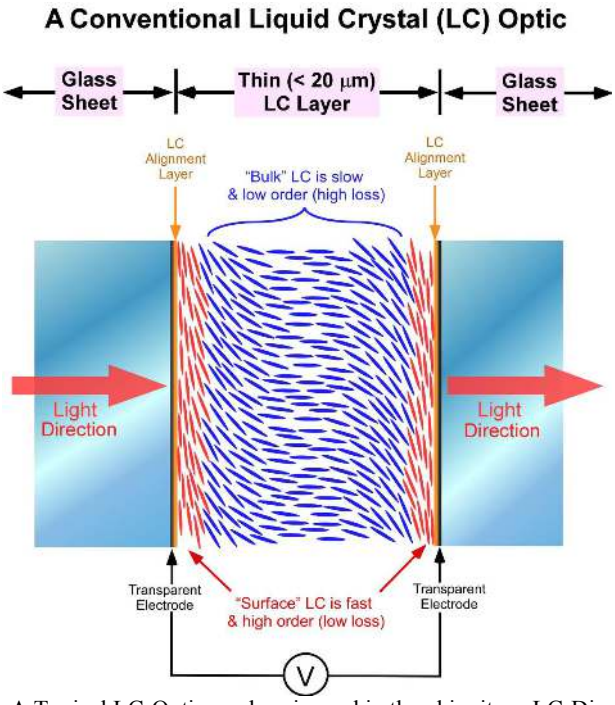

Figure 3: A Typical LC-Optic, such as is used in the ubiquitous LC-Display.

Rather than transmit through an LC cell, which by design must be thin (typically < 20 μm), we utilize the LC as an active cladding layer in a waveguide architecture, i.e., the light skims along the surface of an LC layer, as shown in Figure 4. This *electro-evanescent* architecture circumvents limitations of traditional LC-optics: i) the light never crosses a transparent electrode, ii) the light only interacts with the well-behaved LC-surface layer via the evanescent field, and perhaps most importantly iii) the interaction length is now decoupled from the LC-layer thickness. In this way, the light interacts only with the surface layer of the LC cell, where the molecules are highly ordered (dramatically lower scattering loss) and they respond rapidly to both increases and decreases in electric field (surface mode effect greatly increases the speed, typical relaxation times for LC waveguides are on the order of ***500 μsec***).

Example operation of a basic LC-waveguide is given in Figure 5. In this example a near-IR laser (λ=1.44 μm) is coupled into the waveguide with a polarization such that both the horizontal (TE) and vertical (TM) polarizations are equally filled. These two polarizations are mixed on the output and the voltage on the device is swept. Each time the optical path delay between these two polarization is altered by ½ of an optical wavelength of light the output through the final polarizer goes from a maxima to a minima. This device exhibited nearly 1000 waves of optical path difference control. This translates into greater than 1 mm of voltage tunability over optical phase difference. We know of no other technology that can provide similar voltage control over optical phase. Furthermore, the loss in this waveguide was below our measurement sensitivity of 0.3 dB/cm..

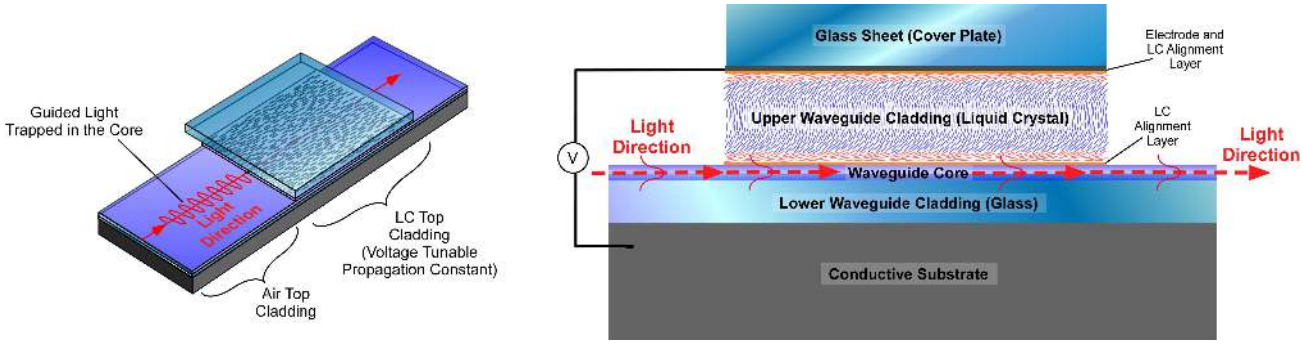

Figure 4 A) The basic geometry of an LC-waveguide. The light is confined to a core and the LC is an electro-optic upper cladding. As the index of refraction of the upper cladding is tuned the "effective index" of the guided mode is also tuned. B) A side view of a liquid crystal waveguide. In a slab waveguide the light is guided in the *x* dimension, but is free to propagate as Gaussian beams, sheets, or even 1D images in the plane.

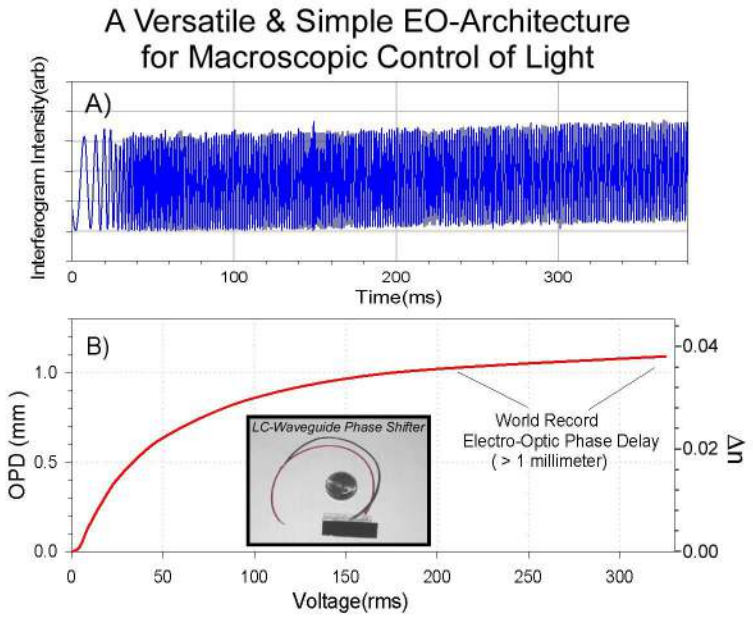

Figure 5 A) The transmission of an LC waveguide between polarizers. The figure was recorded over a longer sweep time so that individual waves could be observed. This is a plot of the relative optical path difference induced by the LC-waveguide, each minima or maxima on the plot corresponds to one wavelength (1.4 μm) of optical phase change. B) The tunable optical phase delay versus applied voltage. For this device *greater than one millimeter* of optical phase delay (OPD) was achieved. The inset shows a picture of the device (next to a nickel for scale).

Below 50 V, the device exhibited $\Delta n_{eff} \sim 0.02$. While this modulation index is several orders of magnitude larger than that for other EO materials, (Typically $\Delta n \approx 10^{-4}$ / KV for EO crystals such as KTP and $LiNbO_3$) detailed theoretical models suggest that this can be even further improved. For a given liquid crystal and waveguide structure, we can model the LC upper cladding and the voltage dependent field profile of the guided light. This is shown in the top of Figure 6. Specifically, our model includes: LC surface energy, pre-tilt, elastic coefficients of the LC, electrical properties of the LC (dielectric constants), optical properties of the LC (birefringence), electrode spacing, and electrical properties of the waveguide materials. With this information we can numerically solve for the LC upper cladding index profile as a function of voltage, following an established routine outlined by S. T. Wu.{Khoo, 1993 #13} Then, for a given index profile we can solve Maxwell's equation for the guided mode and determine the effective index. The index modulation

is the magnitude of the difference between the effective index at zero volts and the effective index and a higher voltage. This model does an excellent job of predicting the experimental results. Furthermore, the model shows that $\Delta n_{eff} = 0.05$ is possible by using highly-birefringent liquid crystals and by keeping the ratio of core thickness to wavelength less than one. While this represents a four-fold decrease in birefringence from the raw liquid crystal, this is more than offset by a possible 10,000-fold increase in the interaction length.

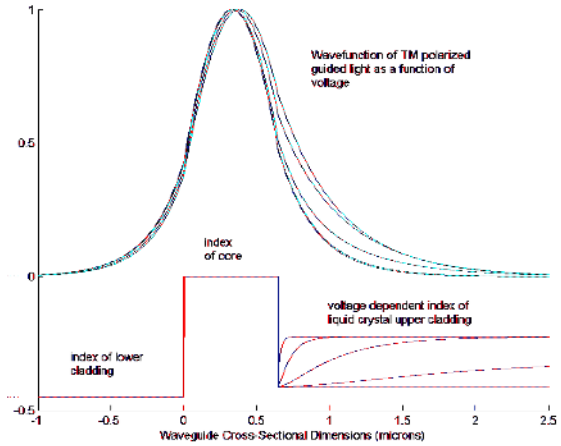

Figure 6: The green lines show the calculated index profile of an LC clad waveguide for different applied voltages. As the voltage is increased the index of the upper cladding also increases. The blue lines show the intensity profile for TM light as a function of voltage. This was obtained by direct solving of Maxwells equations for the waveguide boundary conditions.

The key point is that with $\Delta n_{eff} = 0.05$ it is possible to construct voltage tunable OPD values from 0-1000 waves in a 1 cm waveguide, with wavelengths from visible to several microns. For infrared light at $\lambda = 1$ μm, this translates into a voltage tunable OPD of 0.5 mm per cm of waveguide. Propagation through 10 centimeters of waveguide therefore provides 5 mm of OPD. Integrated optical multipass designs can provide for previously unheard of voltage tunable OPD values from 1 cm up to potentially 10 cm.

2.2. Liquid Crystal Waveguide Interferometer

A schematic of how a LC-waveguide may be used as an interferometer is depicted in Fig 4. Specifically, the light is polarized 45° to the waveguide surface, and therefore equally couples into both the TE and TM modes. An LC waveguide section is used to vary the optical-path-difference (OPD) between the TE and TM modes, which replaces the movable mirror. Finally, the two polarization-separate beams are recombined by means of a polarizer, which is aligned 45° with respect to the waveguide surface. To obtain the interferogram, one varies the OPD between TE and TM modes (via the LC waveguide), and records at the detectors the OPD dependent interference between them. All these elements will be integrated into a monolithic opto-block, thereby eliminating all moving components and surmounting the foremost impediment to FTS miniaturization and cost reduction.

Depicted in Fig. 7 are two detectors. Two detector signals will be phase shifted with respect to one another. Auto-balancing circuits based on the two individual signals ratio-ed to their sum can be used to minimize the impact of source fluctuations. Also not shown are electrodes that are used for active waveguide dispersion compensation. This is key, since optical waveguides possess significant geometric dispersion.

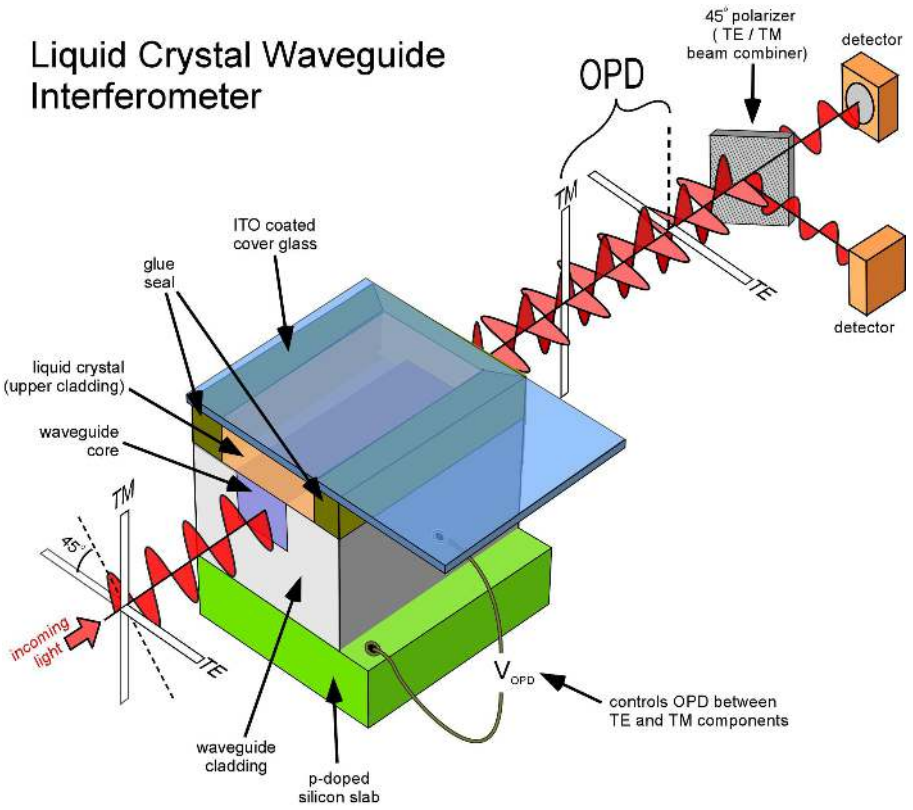

Figure 7: A diagrammatic representation of how a liquid crystal waveguide based interferometer functions. The drawing is not to scale, but rather the waveguide core and cladding size is enhanced for visual clarity. The actual thickness of the waveguide lower cladding (≈8 μm) and core (≈1 μm) is very small. The total length, however, is on the order of 2-10 cm, depending on the desired range of *OPD* values.

2.3. Spectral Resolution

Similar to a conventional FTS, the spectral resolution, $\Delta\sigma$, of the proposed EO-FTS is related to the maximum optical path difference, Δx, or equivalently, the maximum time delay, $\delta_{max,}$ between the two interfering waves: $\Delta\delta = \frac{1}{2\pi OPD} = \frac{1}{2\pi d\left(n_o - n_e\right)}$. Our current LC-waveguide devices have greater than 1 mm of OPD, and we have designs for up to 1 or even 10 cm of OPD in a wrapped channel device. Thus the spectral resolution of <0.3 cm^{-1} (i.e. in sub-nanometer range at about 2μm IR spectral band) can in principle be realized.

3. LC-WAVEGUIDE EO-FTS SENSORS: SYSTEM DESIGN

3.1. Broadband Light Source

Key to a complete FTS sensor system is the appropriate broadband light source. The LC waveguide interferometer requires a high spatial coherence, i.e., all of the light must be confined to the guided mode. In addition to the high *spatial* coherence requirement, low *temporal* coherence is sought, for broadband spectral coverage. While numerous possibilities exist (e.g., halogen lamps, heated elements, LEDs), an especially attractive, very compact and low noise option is provided by super luminescent diodes (SLDs). SLDs with single-mode broadband powers of 10-20 mw are

now commercially available. As an example, companies such as Superlum Diodes, Ltd. provide arrays of five SLDs to provide extended spectral coverage. For greater spectral coverage, this array could incorporate as many SLDs as desired; examples of 32 element diode arrays are given in the literature.{Malinen, 1998 #208}

3.2. Waveguide Design

The waveguide structures that are required for effective LC waveguide OPD control necessitate a tightly confined, high-contrast design. The core or guide layer must have an index that is higher than the LC cladding, i.e., $n_{core} > 1.75$. More specifically, a thin (< 1 μm), high index (n>1.8) core is optimal. The thin core layer pushes a significant fraction of the evanescent wave into the LC cladding, thereby increasing the total achievable electro-optic OPD. The higher index ensures sufficient intensity near the surface layer of the LC, thereby increasing speed and decreasing scattering losses. This need must be balanced with the pragmatic needs of: i) efficient coupling between the light source (be it fiber or other broadband light source), and ii) low loss operation. Vescent Photonics has developed a proprietary waveguide material system that meets these needs. Our waveguide design provides very low waveguide losses of < 0.3 dB/cm and has integrated mode converters that provide very high coupling efficiencies of > 85%. Our waveguide are currently processed on 4 inch silicon wafers. An example of a typical LC-waveguide wafer run is shown in Figure 8. This wafer contains five individual devices.

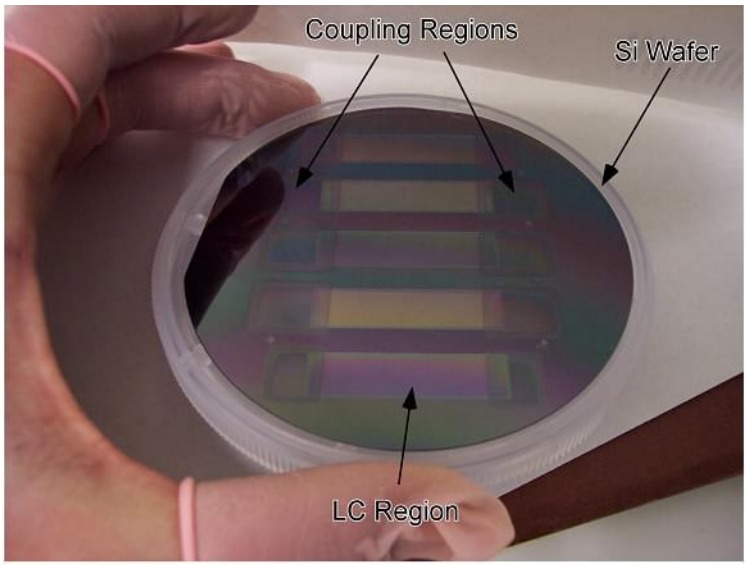

Fig 8. An image of one wafer from a waveguide foundry run. There are five dies on this one wafer. Visible in the picture are the in and out coupling regions (rectangles at the left and right) and the LC region (large rectangle in the middle. The LC interaction region is approximately 4 cm long.

Three different waveguide geometries have been explored for LC-Waveguide FTS devices. These three designs are shown in Figure 9. All three designs incorporate adiabatic mode-converters for efficient light source-to-waveguide couplings. All three designs also incorporate a micro-waveplate, which flips the TE and TM polarization half way through the waveguide, thereby setting the zero OPD point at zero voltage. In order to have a zero optical path difference point, the waveguide must be self compensated. Specifically, the significant geometric birefringence will make the zero voltage point correspond to a large OPD difference point. Stated differently, the TE polarization sees a different optical path than the TM polarization. In order to cancel this out, we insert a ½ waveplate mid-way through the device. This interchanges the TE and TM polarizations, which causes zero voltage on the LC to correspond to a zero optical path delay point. This is the same technique that renders planar waveguide telecom devices, such as arrayed waveguide gratings, polarization independent. While optical waveguides provide compactness and ruggedness, the single mode design also results in significant geometric dispersion, which can wash out the spectral resolution. Therefore, all of the designs also incorporate a proprietary dispersion compensation region. This dispersion compensation region is controlled with a separate electrode via a proprietary algorithm. At the cost of about 20% of the total OPD we have realized dispersion compensation over several 100 nm wide spectral windows.

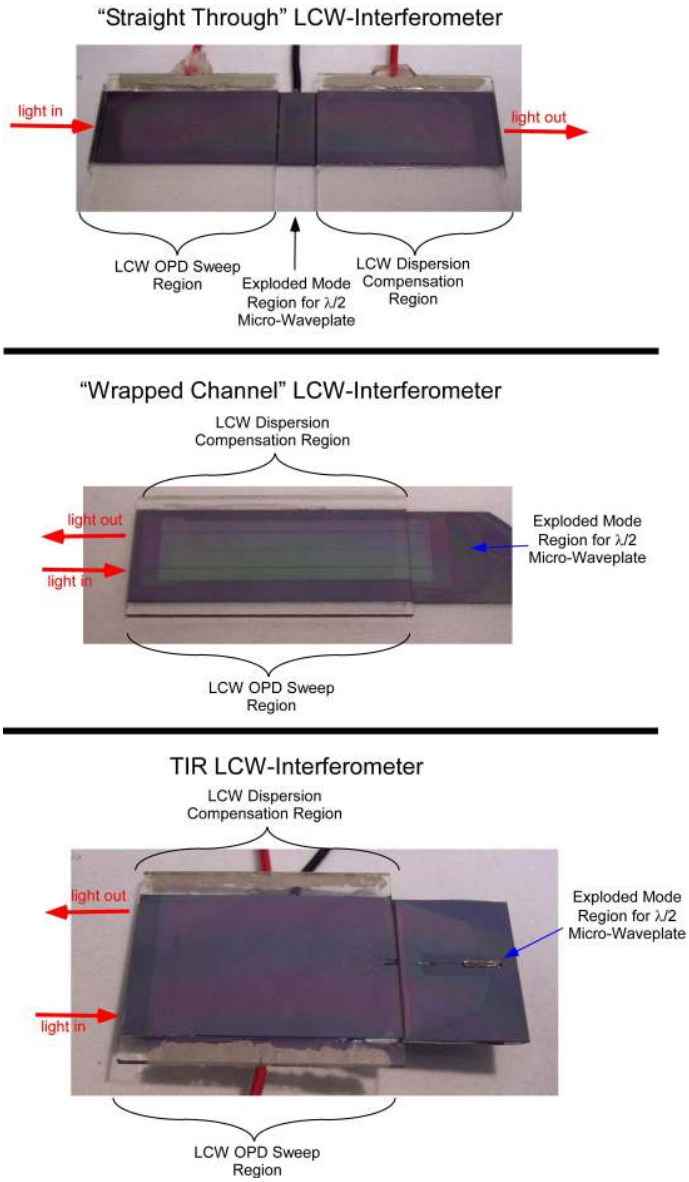

Figure 9 The above figure displays the three waveguide architectures that we are using for LC-Waveguide EO-FTS. All three of them have "exploded mode" input/output regions, wherein the guided beam is expanded to realize more efficient coupling. This exploded mode region is also used for insertion of the half waveplate, which is required for setting of the zero OPD point. The middle figure shows a channel waveguide design. The bottom figure shows a TIR design, with the half waveplate inserted. The top design is a straight-through slab-waveguide approach, with no beam redirection. This design is optically simplier, but the total path length is cut in half, which limits the resolution of the device.

4. PROTOTYPE CONSTRUCTION AND TESTING

A preliminary E-O FTS, operational in the near-IR band, has been built. The current device, along with an exploded view schematic and a total spectrometer system picture, is shown in Figure 10. All of the elements are included, but they are coupled as separate discrete elements. Integration into a monolithic assembly, and utilizing micro-controller electronics, will reduce size/mass and increase durability. This integration is part of the work proposed here.

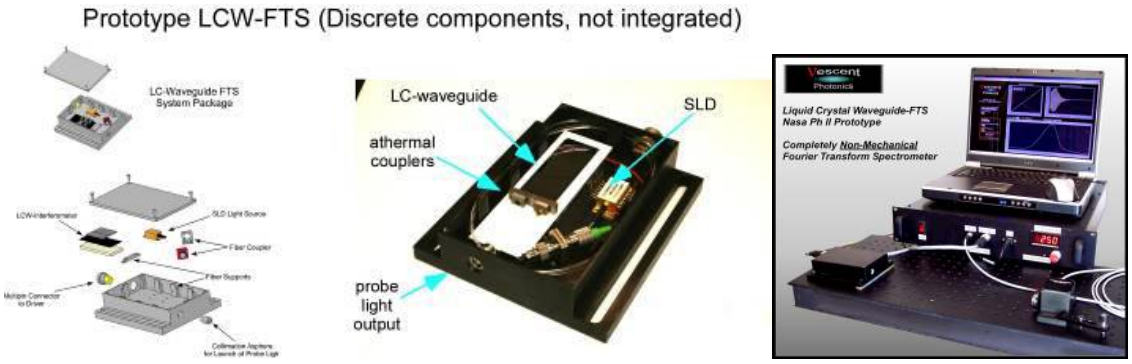

Figure 10: The prototype LC-Waveguide FTS system for operation in the near-IR. This current prototype utilizes a bulky electronics driver and laptop for control and data analysis. This may be replaced with mircro-electronics.

Example performance of a prototype device is shown in Figure 11. The left figure depicts LC-waveguide obtained interferograms of narrow-band light sources. The bottom interferogram is for a single frequency laser. The top

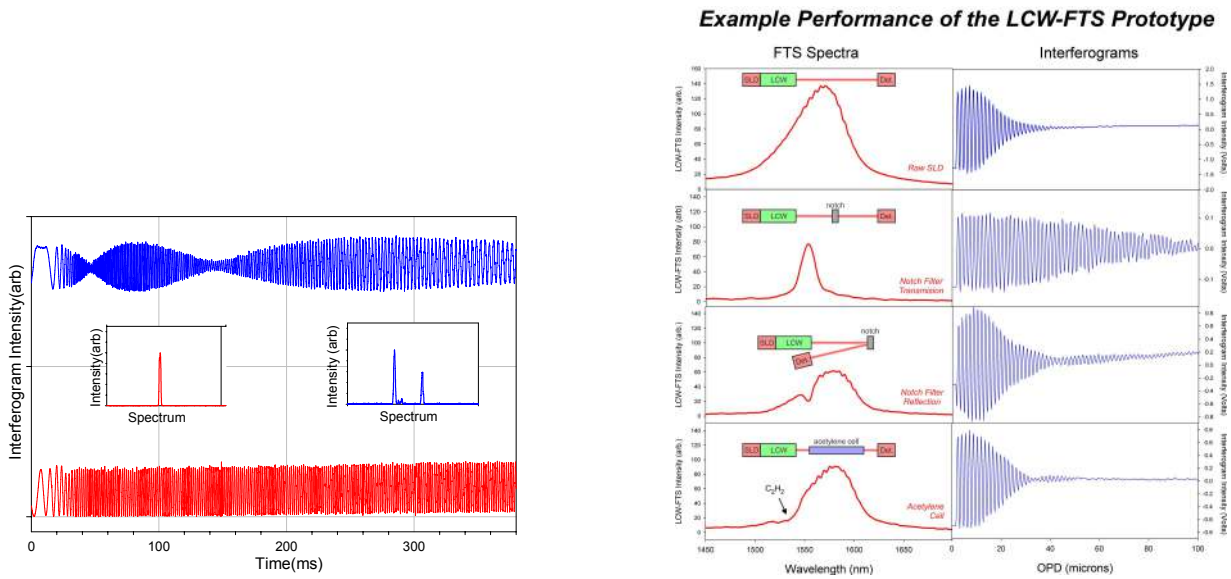

Figure 11. The figure on the left shows an LC waveguide Fourier transform interferogram. The upper trace shows the interferogram (truncated for clarity) of a multimode diode laser. The lower trace shows the interferogram of a pure wavelength source. The "beat-note" for the multimode laser is clearly visible in the top trace. The figure on the right shows the interferogram from a broadband SLD along with the FFT spectra for a variety of absorption features.

interferogram is for two lasers. The beat pattern of the two lasers is clearly visible in the interferogram. The insets show the spectrum of the light sources. The figure on the right shows interferograms and FFT obtained spectra of a broadband SLD with some broadband spectral absorption features. In these experiments both filter and acetylene absorption spectra were recorded. For these current devices the spectral resolution is only about 3-5 nm. Current designs will improve the resolution to <0.5 nm.

5. SUMMARY

The purpose of this research was to develop and construct prototype, miniaturized, robust, and *non-mechanical* Fourier transform spectrometers (FTS), which may ultimately be deployed for either in-situ or remote chemical and spectral analysis. The key innovation for realizing this is our proprietary liquid-crystal (LC) optical waveguide technology, capable of providing an unprecedented, entirely electro-optic replacement for millimeter or even centimeter scale mechanical mirror translation. This LC-waveguide technology, developed by Vescent Photonics, enables a FTS chemical sensor unit completely free of moving components. The ultimate potential attributes of this sensor: i) small size, comparable to a book of matches, ii) low mass, only tens of grams, iii) small energy consumption, $< 10^{-3}$ Watt-hours per measurement, iv) high sensitivity, detectable chemical densities $< 10^{13}$ per cm^3, and v) robust monolithic construction, are aptly suited for future NASA missions. Such a sensor can be integrated and deployed with a variety of exploration platforms. A single device may provide identification and quantification of multiple compounds (e.g., biogenically important CH_4, NH_4, NO_x, H_2O, and many more).

A prototype LC-waveguide FTS sensor was designed and built. The prototype spectrometer is a fully packaged system with a near-IR spectral range from about 1450-1700 nm, with a spectral resolution of 5 nm. The integrated light source is a super-luminescent diode. The system is designed for in-situ analysis, though both remote and reflectance systems are possible. These results and our deliverable demonstrate that LC-waveguide based non-mechanical FTS systems are feasible. Furthermore, engineering improvements to the system will improve the resolution to 0.5 nm and possibly even 0.1 nm, all in a small, low power, and non-mechanical package.

6. ACKNOWLEDGMENTS

The research described in this paper was supported by contracts from both the National Aeronautics and Space Administration and the National Oceanic and Atmospheric Administration.

7. REFERENCES

1. S. P. Davis, M. C. Abrams, and J. W. Brault, *Fourier Transform Spectrometry* (Academic Press, 2001).

2. "http://atmos.jpl.nasa.gov/atmos/pub.list.html."

3. T.-H. Chao, H. Zhou, X. Xia, and S. Serati, "Near IR electro-optic Imaging Fourier Transform Spectrometer," Optical Pattern Recognition XVI, Proceedings of SPIE 5816, 163-171 (2005).

4. I.-C. Khoo, and S.-T. Wu, *Optics and nonlinear optics of liquid crystals* (World Scientific Publishing, 1993).

5. M. Anderson, S. Rommel, and S. Davis, "Liquid Crystal Waveguide for Dynamically Controlling Polarized Light," USPTO, ed. (Vescent Photonics, USA, 2005).

6. M. Anderson, S. Rommel, and S. Davis, "Liquid Crystal Waveguide Having Electric Field Oriented for Controlling Light," USPTO, ed. (Vescent Photonics, USA, 2006).

7. M. Anderson, S. Rommel, and S. Davis, "Liquid Crystal Waveguide Having Two or More Control Voltages for Controlling Polarized Light," USPTO, ed. (Vescent Photonics, USA, 2006).

8. J. Malinen, M. Kansakoski, R. Rikola, and C. G. Eddison, "LED-based NIR spectrometer module for hand-held and process analyser applications," Sensors and Actuators B 51, 220 (1998).